SUPPRESSION OF HEAVY TRUCK DRIVER SEAT VIBRATION USING SLIDING MODE CONTROL & QUANTITATIVE FEEDBACK THEORY

Nuraj I. Rajapakse Graduate student
Gemunu S. Happawana* Assistant Professor
Yildirim Hurmuzlu Professor

Department of Mechanical Engineering
Southern Methodist University, Dallas, TX 75275, USA

Keywords: Nonlinear modeling, Sliding surface, Feedback control, Tracking error, Stability, Time varying surface, Boundary layer, Chattering, Error dynamics, First order filter, and Model uncertainty.

Abstract

This paper presents a robust control method that combines Sliding Mode Control (SMC) and Quantitative Feedback Theory (QFT) for designing a driver seat of a heavy vehicle to reduce driver fatigue. A mathematical model is considered to analyze tracking control characteristics through computer simulation in order to demonstrate the effectiveness of the proposed control methodology. The SMC is used to track the trajectory of the desired motion behavior of the seat. However, when the system enters into sliding regime, chattering occurs due to switching delays as well as vehicle system vibrations. The chattering is eliminated with the introduction QFT inside the boundary layer to ensure smooth tracking. Furthermore, using SMC alone requires higher actuator forces for tracking than using both the control schemes together, causes various problems in selecting hardware. Problems with noise amplification, resonances, presence of uncertainties and unmodeled high frequency dynamics can largely be avoided with the use of QFT over other optimization methods. The main contribution of this paper is to provide the guidance in designing the controller to reduce heavy vehicle seat vibration so that the driver's sensation of comfort maintains a certain level at all times.

NOMENCLATURE

A - Cross sectional area of the hydraulic actuator piston
F_{af} - Actuator force
F_h - Combined nonlinear spring and damper force of the driver seat
k_h - Stiffness of the spring between the seat and the sprung mass
m_h - Mass of the driver and the seat
m_s - Sprung mass
x_h - Vertical position coordinate of the driver seat
x_s - Vertical position coordinate of the sprung mass

* Corresponding Author

1. INTRODUCTION

Relationship between driver fatigue and seat vibration has been used in many literatures based only on anecdotal evidence without doing appropriate research [1, 2]. It is widely believed and proved in field tests, that the lower vertical acceleration levels will increase comfort level of the driver [3-5]. Heavy vehicle truck drivers who usually experience vibration levels around 3

Hz while driving are subjected to fatigue and drowsiness [6]. Lack of concentration while driving leads to road accidents that causes due to fatigue and drowsiness. Most of the early laboratorary and field research revealed and proved this behavior for different road conditions [1-6]. Furthermore, it is strongly believed that intermittent and random vibration can have a stimulating or weakening effect on the driver. Body metabolism and chemistry can largely be affected due to this vibration exposure and result in fatigue [7]. Typical whole-body vibration exposure levels of heavy vehicle drivers are in the range 0.4 m/s^2 - 2.0 m/s^2 with a mean value of 0.7 m/s^2 in the vertical axis [3-6].

Suspension system that links the wheels and the vehicle body determines the ride comfort of the vehicle and its characteristics must be properly evaluated to design a proper driver seat under various operating conditions. A properly designed driver seat causes less driver fatigue and it maintains same vibration level against any external disturbance to provide the best performances in riding. It also improves vehicle control, safety and stability without changing the ride quality and addresses the areas of road holding, load carrying and passenger comfort. Furthermore, it provides directional control during handling maneuvers.

Over the past decades, the application of sliding mode control has been focused in many directions such as the use of sliding control in underwater vehicles, automotive applications and robot manipulators [8-17]. The combination of sliding controllers with state observers was also developed and discussed for both the linear and nonlinear cases [18, 19]. Nonlinear systems are difficult to model as linear systems since there exist some parametric uncertainties and modeling inaccuracies that can eventually resonate the system [9]. The sliding mode control can be used for nonlinear stabilization problems in designing controllers.

In this paper, the sliding mode control theory is applied to track the motion behavior of a driver seat of a heavy vehicle to a trajectory that can reduce driver fatigue and drowsiness. The trajectory is not necessarily be fixed and can be varied accordingly with respect to the driver requirements. This control methodology can overcome most of the road disturbances and provide predetermined seat motion pattern to avoid driver fatigue. However, due to parametric uncertainties and modeling inaccuracies chattering can be observed which causes a major problem in applying SMC alone. In general, the chattering enhances the driver fatigue and also leads to premature failure of controllers. SMC with QFT is a good approach for this kind of problems to eliminate the chattering satisfactorily. Furthermore, it reduces the control effort necessary to maintain the desired motion of the seat and it is broadly discussed in this paper.

2. MATHEMATICAL MODELING

Figure 1 below shows a schematic of a driver seat of a heavy truck. The model is consisting of an actuator, spring, damper and a motor sitting on the sprung mass. The actuator provides actuation force by means of a hydraulic actuator to keep the seat motion within a comfort level for any road disturbance, while the motor maintains desired inclination angle of the driver seat with respect to the roll angle of the sprung mass. Driver seat mechanism is connected to the sprung mass by using a pivoted joint and it provides the flexibility to change the roll angle. The system is equipped with sensors to measure the sprung mass vertical acceleration and roll angle. Hydraulic pressure drop and spool valve displacement are also used as feed back signals.

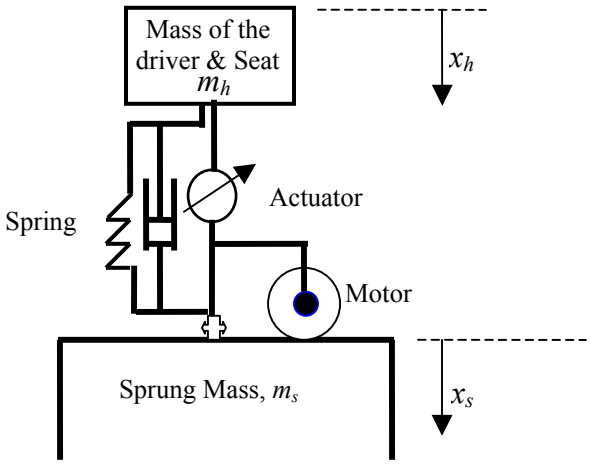

Fig. 1: The driver seat on the sprung mass with supporting devices (Actuator and a motor)

3. EQUATIONS OF MOTION

Based on the mathematical model developed above, the equation of motion in the vertical direction for the driver and the seat can be written as follows:

$$\ddot{x}_h = -(1/m_h)F_h + (1/m_h)F_{af} \qquad (1)$$

Where

$$F_h = k_h(d_h + d_h^{\,3}) + C_h(1 + |\dot{d}_h|^2)\dot{d}_h$$

$$F_{af} = AP_L$$

$$d_h = (x_h - x_s) - a_{1i}\sin\theta_s \quad \text{(see the appendix for details)}$$

In four-way valve-piston hydraulic actuator system, the rate of change of pressure drop across the hydraulic actuator piston, P_L,, is given by:

$$\frac{V_t \dot{P}_L}{4\beta_e} = Q - C_{tp}P_L - A(\dot{x}_h - \dot{x}_s) \qquad (2)$$

Where

V_t – Total actuator volume

β_e – Effective bulk modulus of the fluid

Q – Load flow

C_{tp} – Total piston leakage coefficient

A – Piston area

The load flow of the actuator is given by:

$$Q = \text{sgn}\left[P_s - \text{sgn}(x_v)P_L\right] C_d \omega x_v \sqrt{(1/\rho)\left|P_s - \text{sgn}(x_v)P_L\right|} \qquad (3)$$

Where

P_s – Hydraulic supply pressure

ω – Spool valve area gradient

x_v – Displacement of the spool valve

ρ – Hydraulic fluid density

C_d – Discharge coefficient

Voltage or current can be fed to the servo-valve to control the spool valve displacement of the actuator for generating the force. Moreover, Stiction Model for hydraulic spool can be included to reduce the chattering even further, but it is not discussed here.

4. SLIDING MODE CONTROL PRELIMINARIES

In sliding mode control a time varying surface of S(t) is defined with the use of a desired vector, X_d, and the name is given as the sliding surface. If the state vector, X, can remain on the surface, S(t) for all time, t>0, tracking can be achieved. In other words, problem of tracking the state vector, $X \equiv X_d$ (n-dimensional desired vector) is solved. Scalar quantity, s, is the distance to the sliding surface and this becomes zero at the time of tracking. This replaces the vector X_d effectively by a first order stabilization problem in s. The scalar s represents a realistic measure of tracking performance since bounds on s and the tracking error vector are directly connected together. In designing the controller, a feedback control law U can be chosen appropriately to satisfy sliding conditions. The control law across the sliding surface can be made discontinuous in order to facilitate for the presence of modeling imprecision and of disturbances. Then the discontinuous control law U is smoothed accordingly using QFT to achieve an optimal trade-off between control bandwidth and tracking precision.

Consider the second order single-input dynamic system [9]:

$$\ddot{x} = f(X) + b(X)U \qquad (4)$$

Where

X – State vector, $[x \quad \dot{x}]^T$

x – Output of interest

f – Nonlinear time varying or state dependent function

b – Control gain

U – Control input torque

The control gain, b, can be time varying or state-dependent but is not completely known. In other words, it is sufficient to know the bounding values of b.

$$0 < b_{\min} \le b \le b_{\max} \qquad (5)$$

The estimated value of the control gain, b_{es}, can be found as [2]

$$b_{es} = (b_{\min} b_{\max})^{1/2}$$

Bounds of the gain, b can be written in the form:

$$\beta^{-1} \le \frac{b_{es}}{b} \le \beta \qquad (6)$$

Where

$$\beta = \left[\frac{b_{\max}}{b_{\min}} \right]^{1/2}$$

The nonlinear function f can be estimated (f_{es}) and the estimation error on f is to be bounded by some function of the original states of f.

$$\left| f_{es} - f \right| \le F \qquad (7)$$

In order to have the system track on to a desired trajectory $x(t) \equiv x_d(t)$, a time-varying surface, $S(t)$ in the state-space R^2 by the scalar equation $s(x;t) = s = 0$ is defined.

$$s = \left(\frac{d}{dt} + \lambda \right) \overline{x} = \dot{\overline{x}} + \lambda \overline{x} \qquad (8)$$

Where

$\overline{X} = X - X_d = [\overline{x} \;\; \dot{\overline{x}}]^T$

$\lambda =$ Positive constant (First order filter bandwidth)

When the state vector reaches the sliding surface, $S(t)$, the distance to the sliding surface, s, becomes zero. This represents the dynamics while in sliding mode, such that

$$\dot{s} = 0 \qquad (9)$$

When the Eq. (9) is satisfied, the equivalent control input, U_{eq} can be obtained as follows:

$b \to b_{es}$

$b_{es} U \to U_{es}$

$f \to f_{es}$,

This leads to

$$U_{es} = -f_{es} + \ddot{x}_d - \lambda \dot{\overline{x}}, \text{ and} \qquad (10)$$

U is given by

$$U = \left(\frac{1}{b_{es}} \right) \left(U_{es} - k(x) \operatorname{sgn}(s) \right)$$

Where

k(x) - Control discontinuity

The control discontinuity, *k(x)* is needed to satisfy sliding conditions with the introduction of an estimated equivalent control. However, this control discontinuity is highly dependent on the parametric uncertainty of the system. In order to satisfy sliding conditions and the system trajectories to be remained on the sliding surface, the following must be satisfied.

$$\frac{1}{2}\frac{d}{dt}s^2 = s\dot{s} \le -\eta|s| \qquad (11)$$

Where η is a strictly positive constant.

The control discontinuity can be found from the above inequality:

$$s\left[(f - bb_{es}^{-1}f_{es}) + (1 - bb_{es}^{-1})(-\ddot{x}_d + \lambda\dot{\tilde{x}}) - bb_{es}^{-1}k(x)\,\mathrm{sgn}(s)\right] \le -\eta|s|$$

$$s\left[(f - bb_{es}^{-1}f_{es}) + (1 - bb_{es}^{-1})(-\ddot{x}_d + \lambda\dot{\tilde{x}})\right] + \eta|s| \le bb_{es}^{-1}k(x)|s|$$

$$k(x) \ge \frac{s}{|s|}\left[b_{es}b^{-1}f - f_{es} + (b_{es}b^{-1} - 1)(-\ddot{x}_d + \lambda\dot{\tilde{x}})\right] + b_{es}b^{-1}\eta$$

For the best tracking performance, $k(x)$ must satisfy the inequality as follows:

$$k(x) \ge \left|b_{es}b^{-1}f - f_{es} + (b_{es}b^{-1} - 1)(-\ddot{x}_d + \lambda\dot{\tilde{x}})\right| + b_{es}b^{-1}\eta$$

As seen from the above inequality, the value for $k(x)$ can be simplified further by rearranging f as below:

$f = f_{es} + (f - f_{es})$ and by using $|f_{es} - f| \le F$

$$k(x) \ge \left|b_{es}b^{-1}(f - f_{es}) + (b_{es}b^{-1} - 1)(f_{es} - \ddot{x}_d + \lambda\dot{\tilde{x}})\right| + b_{es}b^{-1}\eta$$

$$k(x) \ge \left|b_{es}b^{-1}(f - f_{es})\right| + \left|(b_{es}b^{-1} - 1)(f_{es} - \ddot{x}_d + \lambda\dot{\tilde{x}})\right| + b_{es}b^{-1}\eta$$

$$k(x) \ge \beta(F + \eta) + (\beta - 1)\left|(f_{es} - \ddot{x}_d + \lambda\dot{\tilde{x}})\right|$$

$$k(x) \ge \beta(F + \eta) + (\beta - 1)|U_{es}| \qquad (12)$$

By choosing $k(x)$ to be large enough, sliding conditions can be guaranteed. This control discontinuity across the surface $s = 0$ increases with the increase of uncertainty of the system parameters. It is important to mention that the functions for f_{es} and F may be thought of as any measured variables external to the system and they also may depend explicitly on time.

5. REARRANGEMENT OF THE SLIDING SURFACE

Sliding condition as in the previous sections, $\dot{s} = 0$ does not necessarily provide smooth tracking performance across the sliding surface. In order to guarantee smooth tracking performance and to design an improved controller, in spite of the control discontinuity, sliding condition can be redefined, i.e. $\dot{s} = -\alpha s$ [8], so that tracking of $x \to x_d$ would achieve an exponential convergence. Here the parameter α is a positive constant. The value for α is determined by considering the tracking smoothness of the unstable system.
This condition modifies U_{es} as follows:

$U_{es} = -f_{es} + \ddot{x}_d - \lambda\dot{\tilde{x}} - \alpha s$ and $k(x)$ must satisfy the condition below.

$$k(x) \geq \left| b_{es}b^{-1}f - f_{es} + (b_{es}b^{-1} - 1)(-\ddot{x}_d + \lambda\dot{\tilde{x}}) \right| + b_{es}b^{-1}\eta - \alpha|s|$$

Further $k(x)$ can be simplified as

$$k(x) \geq \beta(F + \eta) + (\beta - 1)|U_{es}| + (\beta - 2)\alpha|s| \qquad (13)$$

Even though the tracking condition is improved, chattering of the system on the sliding surface is remained as an inherent problem in SMC. This can indeed be removed by using QFT as explained in section 6.

6. QFT CONTROLLER DESIGN

In the previous sections of sliding mode preliminaries, designed control laws, which satisfy sliding conditions, lead to perfect tracking even with some model uncertainties. However, after reaching the boundary layer, the chattering of the controller is observed because of the discontinuity across the sliding surface. In practice this situation extremely complicates designing hardware for the controller. Furthermore, even after designing the controller, a desirable performance could not be achieved because of the time lag of the hardware functionality. Also chattering excites undesirable high frequency dynamics of the system. By using QFT controller, the switching control laws can be modified to eliminate chattering in the system since QFT controller works as a lowpass filter. In QFT, attractiveness of the boundary layer can be maintained for all t >0 by varying the boundary layer thickness, ϕ, as follows:

$$\text{When } |s| \geq \phi \to \frac{1}{2}\frac{d}{dt}s^2 \leq (\dot{\phi} - \eta)|s| \quad [9] \qquad (14)$$

It is evident from Eq. (14) that the boundary layer attraction condition is highly guaranteed in the case of boundary layer contraction ($\dot{\phi} < 0$) than the boundary layer expansion ($\dot{\phi} > 0$). Further more Eq. (14) can be used to modify the control discontinuity gain, $k(x)$, to smoothen the performance by putting $\bar{k}(x)\text{sat}(s/\phi)$ instead of $k(x)\text{sgn}(s)$. Relationship between $\bar{k}(x)$ and $k(x)$ for the boundary layer attraction condition can be presented for both the cases as follows:

$$\dot{\phi} > 0 \to \bar{k}(x) = k(x) - \dot{\phi}/\beta^2 \qquad (15)$$

$$\dot{\phi} < 0 \to \bar{k}(x) = k(x) - \dot{\phi}\beta^2 \qquad (16)$$

Then the control law, U, and $\dot{s}$ become

$$U = \left(\frac{1}{b_{es}}\right)\left(U_{es} - \bar{k}(x)\text{sat}(s/\phi)\right)$$

$$\dot{s} = -bb_{es}^{-1}(\bar{k}(x)\text{sat}(s/\phi) + \alpha s) + \Delta g(x, x_d)$$

Where $\Delta g(x, x_d) = (f - bb_{es}^{-1} f_{es}) + (1 - bb_{es}^{-1})(-\ddot{x}_d + \lambda \dot{\tilde{x}})$

Since $\bar{k}(x)$ and Δg are continuous in x, the system trajectories inside the boundary layer can be expressed in terms of the variable s and the desired trajectory x_d by the following relation: Inside the boundary layer, i.e., $|s| \le \phi \rightarrow \text{sat}(s/\phi) = s/\phi$ and $x \rightarrow x_d$

$$\text{Hence} \quad \dot{s} = -\beta_d^2(\bar{k}(x_d)(s/\phi) + \alpha s) + \Delta g(x_d) \qquad (17)$$

$$\text{Where} \quad \beta_d = \left[\frac{b_{es}(x_d)_{\max}}{b_{es}(x_d)_{\min}}\right]^{1/2}$$

The dynamics inside the boundary layer can be written by combining Eq. (15) and Eq. (16) as follows:

$$\dot{\phi} > 0 \rightarrow \bar{k}(x_d) = k(x_d) - \dot{\phi}/\beta_d^2 \qquad (18)$$

$$\dot{\phi} < 0 \rightarrow \bar{k}(x_d) = k(x_d) - \dot{\phi}\beta_d^2 \qquad (19)$$

By taking the Laplace transform of Equation (17), It can be shown that the variable s is given by the output of a first-order filter, whose dynamics entirely depends on the desired state x_d. $\Delta g(x_d)$ are the inputs to the first order filter, but they are highly uncertain.

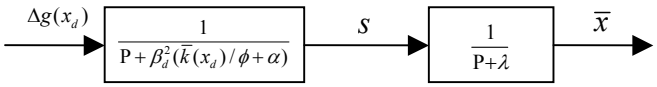

ϕ selection s selection

Fig. 2: Structure of the closed-loop error dynamics

Where P is the Laplace variable. This shows that chattering in the boundary layer due to perturbations or uncertainty of $\Delta g(x_d)$ can satisfactorily be removed by a first order filtering as shown above in the diagram as long as high-frequency unmodeled dynamics are not excited. Further more the boundary layer thickness, ϕ, can be selected as the bandwidth of the first order filter of having input perturbations same as that of the first order filter from the definition of s, which leads to tuning ϕ with λ:

$$\beta_d^2[\bar{k}(x_d)/\phi+\alpha]=\lambda$$
$$\bar{k}(x_d)=(\lambda/\beta_d^2-\alpha)\phi \qquad (20)$$

Combining Eq. (18) and Eq. (20) yields

$$k(x_d)>\phi(\lambda/\beta_d^2-\alpha) \quad \text{and}$$
$$\dot{\phi}+(\lambda-\alpha\beta_d^2)\phi=\beta_d^2 k(x_d) \qquad (21)$$

Also by combining Eq. (19) and Eq. (20) results

$$k(x_d)<\phi(\lambda/\beta_d^2-\alpha) \quad \text{and}$$
$$\dot{\phi}+(\phi/\beta_d^2)[(\lambda/\beta_d^2)-\alpha]=k(x_d)/\beta_d^2 \qquad (22)$$

Equations (15) and (21)

$$\dot{\phi}>0 \rightarrow \bar{k}(x)=k(x)-(\beta_d/\beta)^2[k(x_d)-\phi(\lambda/\beta_d^2-\alpha)] \quad (23)$$

And combining Eq.(13) with Eq. (19)

$$\dot{\phi}<0 \rightarrow \bar{k}(x)=k(x)-(\beta/\beta_d)^2[k(x_d)-\phi(\lambda/\beta_d^2-\alpha)] \quad (24)$$

In addition, initial value of the boundary layer thickness, $\phi(0)$, is given by substituting x_d at t=0 in Eq. (20).

$$\phi(0)=\frac{\bar{k}(x_d(0))}{(\lambda/\beta_d^2)-\alpha}$$

Sections discussed above can be used for applications to track and stabilize highly nonlinear systems. Sliding mode control along with QFT provides better system controllers and it leads to select hardware easier than using SMC alone. The application of this theory to truck driver seat and its simulation are given in the following sections.

7. APPLICATIONS AND SIMULATIONS (MATLAB)

Equation (1) can be represented as,

$$\ddot{x}_h=f+bU \qquad (25)$$

Where

$$f = -(1/m_h)F_h$$

$$b = 1/m_h$$

$$U = F_{af}$$

The expression, f is a time varying function of x_s and the state vector, x_h. The time varying function, x_s can be estimated from the information of the sensor, attached to the sprung mass and its limits of variation must be known. The expression, f and the control gain, b are not required to be known exactly, but their bounds should be known in applying SMC and QFT. In order to perform the simulation, x_s is assumed to vary between -0.3m to 0.3m and it can be approximated by the time varying function, $A\sin(\omega t)$, where ω is the disturbance angular frequency of the road by which the unsprung mass is oscillated. The bounds of the parameters are given as follows:

$$m_{h\min} \le m_h \le m_{h\max}$$

$$x_{s\min} \le x_s \le x_{s\max}$$

$$b_{\min} \le b \le b_{\max}$$

Estimated values of m_h and x_s:

$$m_{hes} = \left|(m_{h\min} m_{h\max})^{1/2}\right|$$

$$x_{ses} = \left(\left|x_{s\min} x_{s\max}\right|\right)^{1/2}$$

Above bounds and the estimated values can roughly be obtained for some heavy trucks by utilizing field test information [20-25]. They are as follows:

$$m_{h\min} = 50\,kg,\ m_{h\max} = 100\,kg,\ x_{s\min} = -0.3\,m,\ x_{s\max} = 0.3\,m,\ \omega = 2\pi(0.1-10)\,rad/s,\ A = 0.3$$

The estimated nonlinear function, f, and bounded estimation error, F, are given by:

$$f_{es} = -(k_h/m_{hes})(x_h - x_{ses})$$

$$F = \left|f_{es} - f\right|_{\max}$$

$$b_{es} = 0.014$$

$$\beta = 1.414$$

$$x_{ses} = \left(\left|(x_s)_{\max} * (x_s)_{\min}\right|\right)^{1/2}$$

The sprung mass is oscillated due to road disturbances and its changing pattern is given by the vertical angular frequency, $\omega = 2\pi(0.1 + |9.9\sin(2\pi t)|)$. This function for ω is used in the simulation in order to vary the sprung mass frequency from 0.1 to 10 Hz. Nevertheless, ω can

be measured by using the sensors in real time and be fed to the controller to estimate the control force necessary to maintain the desired frequency limits of the driver seat. Expected trajectory for x_h is given by the function, $x_{hd} = B\sin\omega_d t$, where ω_d is the desired angular frequency of the driver to have comfortable driving conditions to avoid driver fatigue in the long run. B and ω_d are assumed to be .05 m and $2\pi * 0.5$ rad/s during the simulation which yields 0.5 Hz continuous vibration for the driver seat over the time. Furthermore, Mass of the driver and seat is considered as 70 kg throughout the simulation. This value changes from driver to driver and can be obtained by the attached load cell to the driver seat to calculate the control force. Spring constant between the driver seat and the sprung mass is selected as 100 N/m in obtaining plots. It is important to mention that, this control scheme provides sufficient room to change the vehicle parameters of the system according to the driver requirements to achieve ride comfort.

8. USING SLIDING MODE ONLY

In this section the tracking is achieved by using SMC alone and the simulation results are obtained as follows:

Consider $x_h = x(1)(m)$ and $\dot{x}_h = x(2)(m/s)$. The Eq. (25) is represented in state space form as follows:

$$\dot{x}(1) = x(2)$$

$$\dot{x}(2) = -\left(k_h / m_h\right)\left(x(1) - x_{ses}\right) + bU$$

Combining Eq. (8), Eq. (10) and Eq. (25), estimated control law becomes,

$$U_{es} = -f_{es} + \ddot{x}_{hd} - \lambda[x(2) - \dot{x}_{hd}]$$

Figure 3 to Fig. 6 shows system trajectories, tracking error and control torque for the initial condition: $[x_h, \dot{x}_h]$=[0.1m , 1m/s.] using the control law. Figure 3 provides the tracked vertical displacement of the driver seat vs. time and perfect tracking behavior can be observed. Figure 4 exhibits the tracking error and it is enlarged in Fig. 5 to show it's chattering behavior after the tracking is achieved. Chattering is undesirable for the controller that makes impossible in selecting hardware and leads to premature failure of hardware.

The values for λ and η in Eq. (8) and Eq. (11) are chosen as 20 and 0.1[9] to obtain the plots and to achieve satisfactory tracking performance. The sampling rate of 1 kHz is selected in the simulation. $\dot{s} = 0$ condition and the *signum* function are used. The plot of control force vs. time is given in Fig. 6. It is very important to mention that, the tracking is guaranteed only with excessive control forces. Mass of the driver and driver seat, limits of it's operation, control bandwidth, initial conditions, sprung mass vibrations, chattering and system uncertainties are various factors that cause to generate huge control forces. It is worthwhile to mention that this selected example is governed only by the linear equations with sine disturbance function, which cause for the controller to generate periodic sinusoidal signals. In general, the road disturbance is sporadic and the smooth control action can never be expected. This will lead to chattering and QFT is needed to filter them out. Moreover, applying SMC with QFT can reduce excessive control forces and will ease the selection of hardware.

In subsequent results, the spring constant of the tires is selected as 1200kN/m and the damping coefficient as 300kNs/m. Some of the trucks' numerical parameters [8, 12] are used in obtaining plots and they are listed below:

m_h=100kg, m_s=3300kg, m_u=1000kg, k_s = 200 kN/m, k_h = 1 kN/m, C_s = 50 kNs/m, C_h = 0.4 kNs/m, J_s = 3000 kgm^2 , J_u = 900 kgm^2, A_i = 0.3 m, S_i=0.9 m, and a_{1i} = 0.8 m.

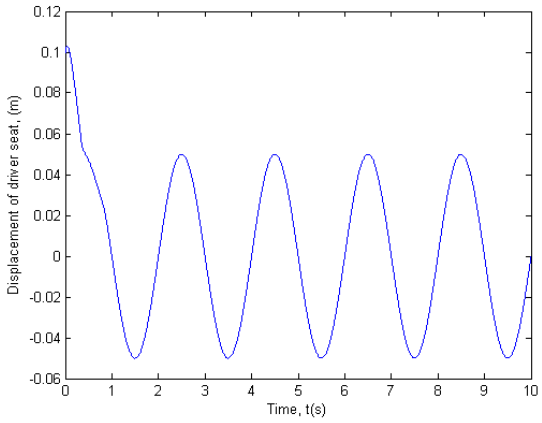

Fig. 3: Vertical displacement of driver seat vs. time

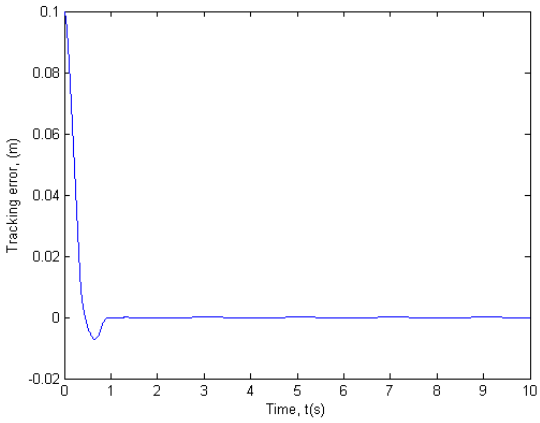

Fig. 4: Tracking error vs. time

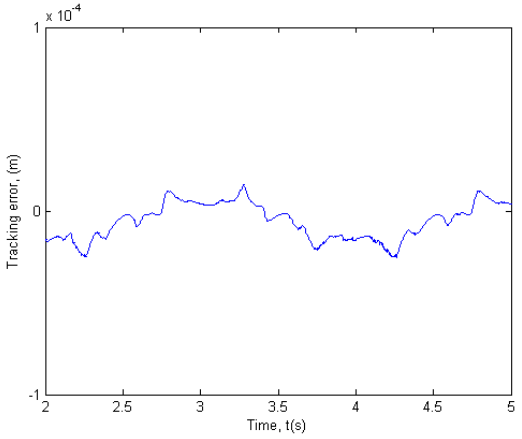

Fig. 5: Zoomed in tracking error vs. time

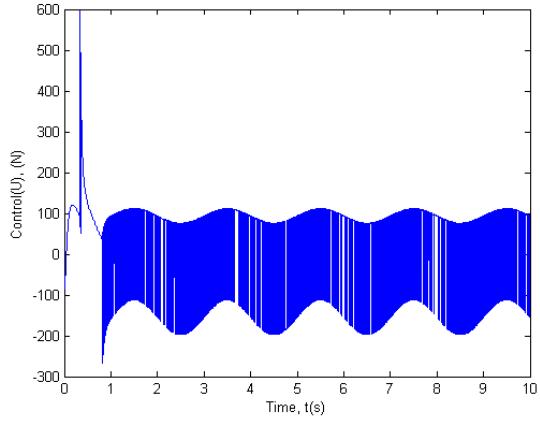

Fig. 6: Control force vs. time

9. USE OF QFT ON THE SLIDING SURFACE

In order to lower the excessive control force and to further smoothen the control behavior with a view of reducing chattering, QFT is introduced in side the boundary layer. The following graphs are plotted for the initial boundary layer thickness of 0.1 meters.

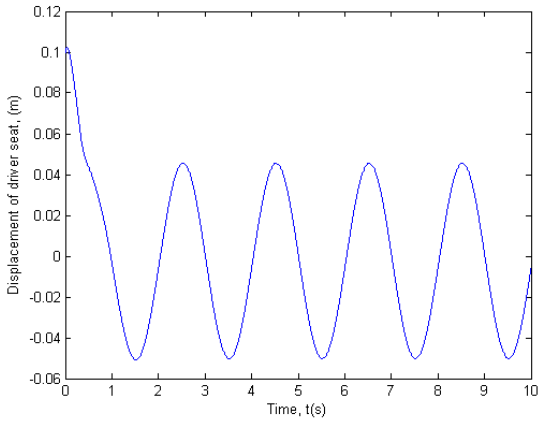

Fig. 7: Vertical displacement of driver seat vs. time

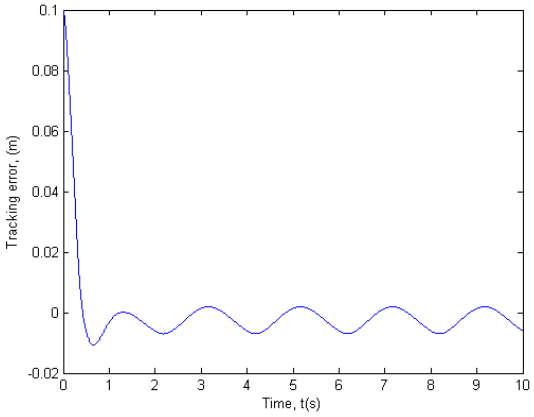

Fig. 8: Tracking error vs. time

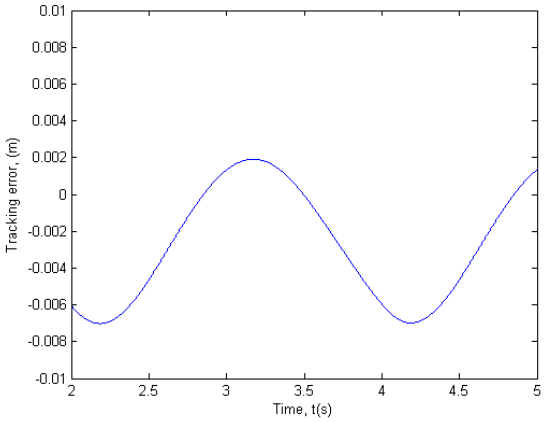

Fig. 9: Zoomed in tracking error vs. time

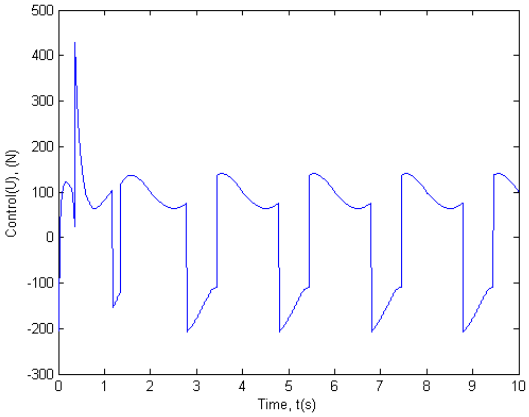

Fig. 10: Control force vs. time

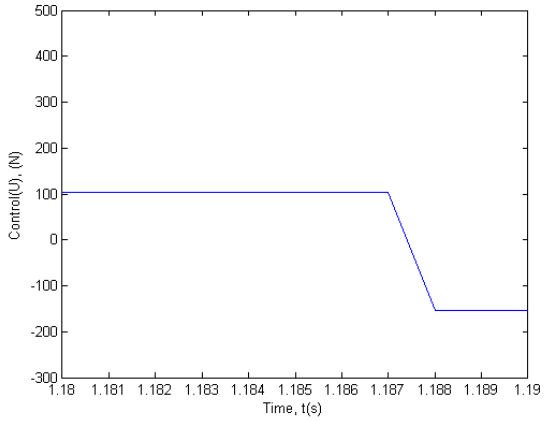

Fig. 11: Zoomed in control force vs. time

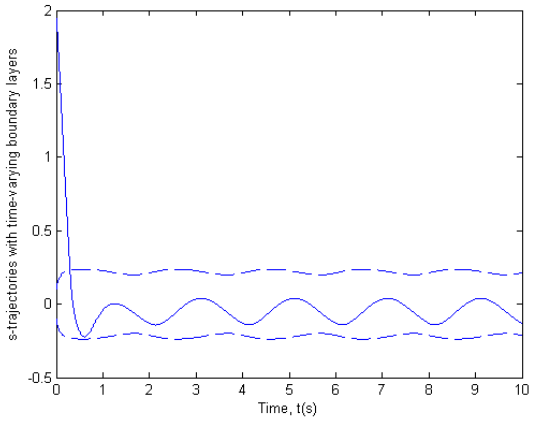

Fig. 12: s-trajectory with time-varying boundary layer vs. time

Figure 7 again shows that the system is tracked to the trajectory of interest and it follows the desired trajectory of the seat motion over the time. Figure 9 provides zoomed in tracking error of Fig. 8 which is very small and perfect tracking condition is achieved. The control force needed to track the system is given in Fig. 10. Figure 11 provides control forces for both the cases, i.e. SMC with QFT and SMC alone. SMC with QFT yields lower control force and this can precisely be generated by using a hydraulic actuator. Increase of the parameter λ will decrease the tracking error with the increase of initial control effort.

Varying thickness of the boundary layer allows the better use of the available bandwidth, which causes to reduce the control effort for tracking the system. Parameter uncertainties can effectively be addressed and the control force can be smoothened with the use of both the SMC and QFT rather than applying SMC alone. Furthermore, a successful application of QFT methodology requires selecting suitable function for F, since the change in boundary layer thickness is dependent on the bounds of F. Increase of the bounds of F will increase the boundary layer thickness that leads to overestimate the change in boundary layer thickness and the control effort. Evolution of dynamic model uncertainty with time is given by the change of boundary layer thickness. Right selection of the parameters and their bounds always result in lower tracking errors and control forces, which will ease choosing hardware for most of the applications.

10. CONCLUSIONS

This paper provides adequate information in designing a road adaptive driver seat of a heavy truck via a combination of SMC and QFT. Based on the assumptions, the simulation shows that these adaptive driver seat controllers provide superior driver comfort over a wide range of road disturbances. However, Parameter uncertainty, the presence of unmodeled dynamics such as structural resonant modes, neglected time-delays and finite sampling rate can largely change the dynamics of these systems. SMC provides effective methodology to design and test the controllers in the performance trade-offs, thus the tracking is guaranteed within the operating limits of the system. Combine use of SMC and QFT facilitates the controller to behave smoothly and with minimum chattering that is an inherent obstacle of using SMC alone. Chattering reduction by the use of QFT supports in selecting hardware and also to reduce excessive control action. In this paper simulation study is done for a linear system with sinusoidal disturbance inputs. It is seen that very high control effort is needed due to fast switching behavior in the case of using SMC alone. QFT smoothens the switching nature and the control effort can be minimized. Most of the controllers fail when excessive chattering is present and SMC with QFT can be used effectively to smoothen the control action. Furthermore, in this example control gain is fixed and it is independent of the states. This will ease the control manipulation. But, this is not the case in many situations where chattering is most likely the problem. This developed theory can be used effectively in most of the control problems to reduce chattering and to lower the control effort. To mention one thing particularly is that the acceleration feedback is not always needed for position control, but it depends mainly on the control methodology and the system employed. Here, we haven't discussed other seat control methods and their trade offs. In order to implement the control law, the road disturbance frequency, ω should be measured at a rate more than 1000Hz (just to comply with the simulation requirements) to update the system, but higher the better. The bandwidth of the

actuator depends upon several factors, i.e. how quickly the actuator can generate the force needed, road profile, response time, and signal delay etc.

Driver fatigue is a contributing factor in between 4 to 30 percent of road crashes and the low frequency vibrations in heavy vehicles are mostly caused by the long wavelengths of the road surface. These wavelengths occur on roads creating an undulating effect. Valuable scientific data on Physiological and psychological effects are needed to develop guidelines for better truck seat designs. This approach can easily be adopted for most of the designs and provide satisfactory results to reduce driver fatigue and drowsiness.

11. REFERENCES

[1] L. J. Wilson and T. W. Horner, " Data Analysis of Tractor-Trailer Drivers to Assess Drivers' Perception of Heavy Duty Truck Ride Quality ", Report DOT-HS-805-139, National Technical Information Service, Springfield, VA, USA, 1979.

[2] J. M. Randall, " Human subjective response to lorry vibration: implications for farm animal transport " , J. Agric. Engng, Res, Vol 52, pp. 295-307, 1992.

[3] U. Landstrom and R. Landstrom, " Changes in wakefulness during exposure to whole body vibration ", Electroencephal, Clin, Neurophysiol, Vol 61, pp. 411-115, 1985.

[4] A.O. Altunel, " The effect of low-tire pressure on the performance of forest products transportation vehicles ", Master's thesis, Louisiana State University, School of Forestry, Wildlife and Fisheries, 1996.

[5] A.O. Altunel and C. F. de Hoop, " The Effect of Lowered Tire Pressure on a Log Truck Driver Seat ", Louisiana State University Agric. Center, Baton Rouge, USA, Vol. 9, no. 2, 1998.

[6] N. Mabbott, G. foster and B. Mcphee, " Heavy Vehicle Seat Vibration and Driver Fatigue ", Australian Transport Safety Bureau, Report No. CR 203, pp. 35, 2001.

[7] Y. Kamenskii and I. M. Nosova, " Effect of whole body vibration on certain indicators of neuro-endocrine processes ", Noise and Vibration Bulletin, pp. 205-206, 1989.

[8] E. Z. Taha, G. S. Happawana and Y. Hurmuzlu, " Quantitative feedback theory (QFT) for chattering reduction and improved tracking in sliding mode control (SMC) ", ASME J. of Dynamic Systems, Measurement, and Control, Vol. 125, pp 665- 669, 2003.

[9] E. S. Jean-Jacques and L. Weiping, Applied Nonlinear Control, Prentice-Hall, Inc., Englewood Cliffs, New Jersey 07632, 1991.

[10] J. K. Roberge, " The mechanical seal ", Bachelor's thesis, Massachusetts Institute of Technology, 1960.

[11] R. C. Dorf, Modern Control Systems, Addison-Wesley, Reading, Massachusetts, pp. 276 – 279, 1967.

[12] K. Ogata, Modern Control Engineering, Prentice-Hall, Englewood Cliffs, New Jersey, pp. 277 – 279, 1970.

[13] D. T. Higdon and R. H. Cannon, ASME J. of the Control of Unstable Multiple-Output Mechanical Systems, ASME Publication 63-WA-148, New York, 1963.

[14] J. G. Truxal, State Models, Transfer Functions, and Simulation, Monograph 8, Discrete Systems Concept Project, 1965.

[15] K. H. Lundberg and J. K. Roberge, " Classical dual-inverted-pendulum control " In Proceeding of the IEEE CDC 2003, Maui, Hawaii, pp. 4399-4404, 2003.

[16] L. C. Phillips, " Control of a dual inverted pendulum system using linear-quadratic and H-infinity methods ", Master's thesis, Massachusetts Institute of Technology, 1994.

[17] W. McC. Siebert, Circuits, Signals, and Systems, MIT Press, Cambridge, Massachusetts, 1986.

[18] J. K. Hedrick and S. Gopalswamy, Nonlinear Flight Control Design via Sliding Method, Dept. of Mechanical Engineering, Univ. of California, Berkely, 1989.

[19] A. G. Bondarev, S. A. Bondarev, N. Y. Kostylyova and V. I. Utkin, Sliding Modes in Systems with Asymptotic State Observers, Autom. Remote Contr., 6, 1985.

[20] B. Tabarrok, X. Tong, " Directional Stability Analysis of Logging Trucks by a Yaw Roll Model ", Technical Reports, University of Victoria, Mechanical Engineering Department, pp. 57- 62, 1993

[21] T. D. Gillespie, Fundamentals of Vehicle Dynamics, SAE, Inc. Warrendale, PA, 1992.

[22] E. Esmailzadeh, L. Tong. and B. Tabarrok, " Road Vehicle Dynamics of Log Hauling Combination Trucks ", SAE Technical Paper Series 912670, pp. 453-466, 1990.

[23] J.Y. Wong, Theory of Ground Vehicles, New York, N.Y., John Wiley and Sons, 1978.

[24] B. Tabarrok, and L. Tong, " The Directional Stability Analysis of Log Hauling Truck – Double Doglogger ", Technical Reports, University of Victoria, Mechanical Engineering Department, DSC-Vol. 44, pp. 383-396, 1992.

[25] P.V. Aksionov, " Law and criterion for evaluation of optimum power distribution to vehicle wheels ", Int. J. Vehicle Design, Vol. 25, No. 3, pp. 198-202, 2001.

APPENDIX

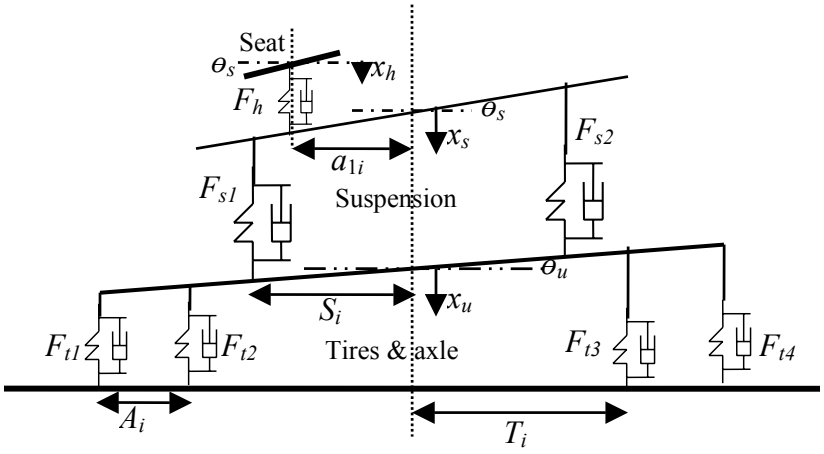

Fig. 13: Five-degree-of-freedom roll and bounce motion configuration of the system to a sudden impact

COMMON EQUATION FOR REPRESENTING NONLINEAR FORCE

Nonlinear tire forces, suspension forces, and driver seat forces can be obtained by substituting appropriate coefficients to the following nonlinear equation that covers wide range of operating conditions for representing dynamical behavior of the system.

$$F = k(d + d^3) + C(1 + |\dot{d}|^2)\dot{d}$$

Where

F – Force

k – Spring constant

C – Damping coefficient

d – Deflection

$\dot{d}$ – Rate of change of deflection

For the suspension:

$$F_{si} = k_{si}(d_{si} + d_{si}^{\ 3}) + C_{si}(1 + |\dot{d}_{si}|^2)\dot{d}_{si} \quad , i = 1,2$$

For the tires:

$$F_{ti} = k_{ti}(d_{ti} + d_{ti}^{\ 3}) + C_{ti}(1 + |\dot{d}_{ti}|^2)\dot{d}_{ti} \quad , i = 1,2,3,4$$

For the seat:

$$F_h = k_h(d_h + d_h^{\ 3}) + C_h(1 + |\dot{d}_h|^2)\dot{d}_h$$

DEFLECTION OF THE SUSPENSION SPRINGS AND DAMPERS

Based on the mathematical model developed, deflection of the suspension system on the axle is found for both sides as follows:

$$\text{Deflection of side 1, } d_{s1} = (x_s - x_u) + S_i(\sin\theta_s - \sin\theta_u)$$
$$\text{Deflection of side 2, } d_{s2} = (x_s - x_u) - S_i(\sin\theta_s - \sin\theta_u)$$

DEFLECTION OF THE SEAT SPRINGS AND DAMPERS

By considering the free body diagram in Fig. 13, deflection of the seat is obtained as follows:

$$d_h = (x_h - x_s) - a_{1i}\sin\theta_s$$

TIRE DEFLECTIONS

The tires are modeled by using springs and dampers. Deflections of the tires to a road disturbance are given by the following equations.

$$\text{Deflection of tire 1, } d_{t1} = x_u + (T_i + A_i)\sin\theta_u$$
$$\text{Deflection of tire 2, } d_{t2} = x_u + T_i\sin\theta_u$$
$$\text{Deflection of tire 3, } d_{t3} = x_u - T_i\sin\theta_u$$
$$\text{Deflection of tire 4, } d_{t4} = x_u - (T_i + A_i)\sin\theta_u$$

EQUATIONS OF MOTION

Based on the mathematical model developed above, the equations of motion for each of the sprung mass, unsprung mass, and the seat are written by utilizing the free-body diagram of the system in Fig. 13 as follows:

Vertical and roll motion for the i^{th} axle (unsprung mass)

$$m_u\ddot{x}_u = (F_{s1} + F_{s2}) - (F_{t1} + F_{t2} + F_{t3} + F_{t4}) \quad (26)$$

$$J_u\ddot{\theta}_u = S_i(F_{s1} - F_{s2})\cos\theta_u + T_i(F_{t3} - F_{t2})\cos\theta_u + (T_i + A_i)(F_{t4} - F_{t1})\cos\theta_u \quad (27)$$

Vertical and roll motion for the sprung mass

$$m_s\ddot{x}_s = -(F_{s1} + F_{s2}) + F_h \quad (28)$$

$$J_s\ddot{\theta}_s = S_i(F_{s2} - F_{s1})\cos\theta_s + a_{1i}F_h\cos\theta_s \quad (29)$$

Vertical motion for the seat

$$m_h\ddot{x}_h = -F_h \quad (30)$$

Equations (26)-(30) have to be solved simultaneously, since there exist many parameters and nonlinearities. Nonlinear effects can better be understood by varying the parameters and

examining relevant dynamical behavior, since changes in parameters change the dynamics of the system. Furthermore, Equations (26)-(30) can be represented in the phase plane, while varying the parameters of the truck, since each and every trajectory in the phase portrait characterizes the state of the truck. Equations above can be converted to the state space form and the solutions can be obtained using MATLAB. Phase portraits are used to observe the nonlinear effects with the change of the parameters. Change of initial conditions clearly changes the phase portraits and the important effects on the dynamical behavior of the truck can be understood.